

## Higgs boson searches beyond the Standard Model

---

**Claudio Caputo**<sup>\*†</sup>

*Università degli Studi di Bari, Istituto Nazionale di Fisica Nucleare*

*E-mail:* [claudio.caputo@cern.ch](mailto:claudio.caputo@cern.ch)

**Paolo Francavilla**<sup>‡</sup>

*Laboratoire de Physique Nucléaire et de Hautes Energies and Institute Lagrange de Paris,*

*E-mail:* [paolo.francavilla@cern.ch](mailto:paolo.francavilla@cern.ch)

.....

*VII Workshop italiano sulla fisica pp a LHC*

*16-18 Maggio 2016*

*Pisa, Italy*

---

<sup>\*</sup>Speaker.

<sup>†</sup>A footnote may follow.

<sup>‡</sup>This work is partially supported by the ILP LABEX (under reference ANR-10-LABX-63 and ANR-11-IDEX-0004-02).

## 1. Introduction

Following the discovery of a scalar particle at the Large Hadron Collider (LHC), an important question is whether this is the Standard Model (SM) Higgs boson or part of an extended Higgs sector. One interesting approach to answer this question is to search for additional scalars, whose observation could confirm existence of an extended Higgs sector. For the first LHC collision data provided at a centre-of-mass energy of 13 TeV and recorded by the ATLAS and CMS detectors, the collaborations have performed many searches that are motivated by a variety of models beyond the SM. The simplest extensions of the SM involve the addition of an additional singlet or doublet field, known as Electroweak Singlet Models (EWS) and Two-Higgs-Doublet Models (2HDM), respectively. Many searches are motivated by these extensions and benchmarks within specific related models, such as the Minimal Supersymmetric Standard Model (MSSM). The MSSM in a particular benchmark scenario is completely determined by two parameters, the mass of one of the Higgs bosons and the ratio of the vacuum expectation values,  $\tan\beta$ . In figure 1 is shown the Run1 results by ATLAS and CMS collaborations [12, 8].

This proceeding will detail the wide variety of new searches performed with the 13 TeV data, which are performed with an integrated luminosity of  $3.2 \text{ fb}^{-1}$  and up to  $2.8 \text{ fb}^{-1}$  with the ATLAS [2, 11, 4, 9, 10] and CMS [5, 6, 7] detectors, respectively. Several recent results with the 8 TeV dataset were also presented [17, 16, 15, 3] [13], but will not be discussed here.

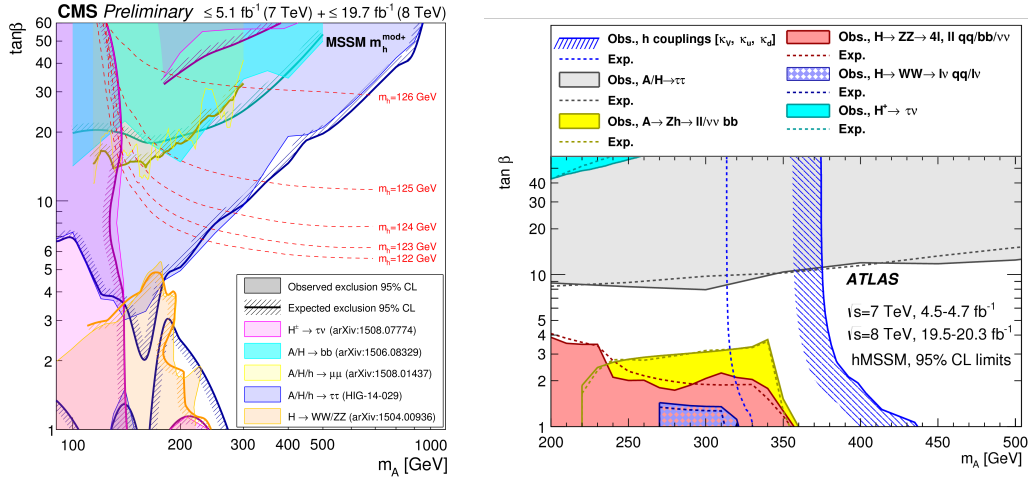


**Figure 1:** Run1  $m_A - \tan\beta$  exclusion plane by (left) CMS experiment and (right) ATLAS experiment.

## 2. Search for neutral Higgs bosons $H/A \rightarrow \tau\tau$

For extensions of the Higgs sector containing two Higgs doublets, the couplings of the heavy Higgs bosons to down-type fermions can be enhanced with respect to the SM for large  $\tan\beta$  values (the ratio of the vacuum expectation values of the two Higgs doublets). This results in increased branching fractions to  $\tau$  leptons and  $b$  quarks, as well as a higher cross section for Higgs boson production in association with  $b$ -quarks. This has motivated a variety of searches in  $\tau\tau$  and  $b\bar{b}$  final states at LEP [29], the Tevatron [30–32] and the LHC -Run1 [33–38], with no indication of an excess over the expected SM background.

The ATLAS collaboration the CMS collaboration have performed searches for neutral Higgs bosons decaying to  $\tau$  leptons using proton–proton collision data collected at a centre-of-mass energy of 13 TeV in 2015, corresponding to an integrated luminosity of 3.2 fb<sup>-1</sup> and 2.3 fb<sup>-1</sup> respectively. The search is performed in three channels by the ATLAS collaboration: the  $\tau_e\tau_{\text{had}}$  channel where one  $\tau$  decays leptonically to an electron and neutrinos and the other hadronically (to hadrons and a neutrino), the  $\tau_\mu\tau_{\text{had}}$  channel where the leptonically decaying  $\tau$  produce a muon and neutrinos, and the  $\tau_{\text{had}}\tau_{\text{had}}$  channel where both  $\tau$  leptons decay hadronically. In addition to the previous three channels, the CMS collaboration extended the search in the  $\tau_e\tau_\mu$  channel in which both the  $\tau$  decay leptonically. In addition, the CMS collaboration divided the events into two categories based on the number of b-tagged jets: events with exactly zero b tagged jets and events with at least one b tagged jet.

### 2.1 $\tau_{\text{had}}$ reconstruction

For these analyses, the reconstruction and the identification of hadronic decays of  $\tau$  leptons is critical. The hadronic decays of  $\tau$  leptons are predominantly characterized by the presence of one or three charged particles, accompanied by a neutrino and possibly neutral pions. In ATLAS, the reconstruction of their visible decay products, hereafter referred to as  $\tau_{\text{had-vis}}$ , starts with jets reconstructed from topological clusters in the calorimeter using the anti-kt algorithm with a size parameter value  $\Delta R = 0.4$  [78]. The  $\tau_{\text{had-vis}}$  candidate must have energy deposits in the calorimeters in the range  $|\eta| < 2.5$ , with the transition region between the barrel and end-cap calorimeters ( $1.37 < |\eta| < 1.52$ ) excluded, have a transverse momentum greater than 20 GeV, one or three associated tracks and an electric charge of  $\pm 1$ . A multivariate Boosted Decision Tree (BDT) based identification is used to reject backgrounds from jets, using shower shape and track multiplicity properties of true  $\tau_{\text{had-vis}}$  objects in the MC. An additional dedicated likelihood-based veto is used to reduce the number of electrons misidentified as  $\tau_{\text{had-vis}}$ . In the ATLAS analysis, two  $\tau_{\text{had-vis}}$  identification selections are used: "loose" and "medium" with efficiencies for true  $\tau_{\text{had-vis}}$  objects of about 65% and 55%, respectively. In CMS, hadronically decaying  $\tau$  leptons are reconstructed using the hadron-plus-strips algorithm [37]. The algorithm considers candidates with one charged pion and up to two neutral pions, or three charged pions, and is seeded by a jet. The neutral pions decay rapidly into two photons, and are reconstructed as "strips" of electromagnetic particles, formed with dynamic size from energy depositions in the electromagnetic calorimeter ECAL. The  $\tau$  decay mode is reconstructed by combining the charged hadrons with the ECAL strips. The  $\tau$  candidate must have  $|\eta| < 2.3$  and a transverse momentum greater than 20 GeV for the  $\tau_e\tau_{\text{had}}$  and  $\tau_\mu\tau_{\text{had}}$  channels, while  $|\eta| < 2.1$  and  $p_T > 40$  GeV for the  $\tau_{\text{had}}\tau_{\text{had}}$  channel. The  $\tau_{\text{had}}$  candidates that

are also compatible with muons or electrons are rejected. Jets originating from the hadronization of quarks and gluons are suppressed by requiring the  $\tau_{\text{had}}$  candidate to be isolated, where the isolation variable is computed using a multivariate (MVA) approach [37]. This is particularly useful in high mass searches where the remaining background is almost entirely due to such fakes.

## 2.2 The $\tau_{\text{had}}\tau_{\text{had}}$ , $\tau_e\tau_{\text{had}}$ , $\tau_\mu\tau_{\text{had}}$ and $\tau_e\tau_\mu$ channels

In the  $\tau_{\text{had}}\tau_{\text{had}}$  channel, multi-jet events form the dominant background, and they are estimated using a data-driven fake-factor method in ATLAS, while is calculated using events in data with slightly looser isolation conditions compared with the signal  $\tau_{\text{had}}$ . These events are then weighted by the extrapolation factor from the nominal selection to this control region as measured in data events with  $\tau_{\text{had}}$  candidate having the same charge. Events from other processes with a jet misidentified as a  $\tau_{\text{had}}$ , such as  $W$ +jets and top-quark backgrounds, are taken from simulation and, in ATLAS, corrected using fake rates measured from data. Events with correctly identified  $\tau_{\text{had}}$  are taken from simulation, with additional derived data/MC corrections.

In the  $\tau_e\tau_{\text{had}}$  and  $\tau_\mu\tau_{\text{had}}$  channels, the background is composed by processes involving jets misidentified as  $\tau_{\text{had}}$  (multi-jet,  $W$ +jets), processes with electrons misidentified as a  $\tau_{\text{had}}$  ( $Z/\gamma \rightarrow ee$ ), and backgrounds with a correctly identified  $\tau_{\text{had}}$  ( $Z/\gamma \rightarrow \tau\tau$  or  $t\bar{t} \rightarrow W^+W^-b\bar{b} \rightarrow l\tau_{\text{had}}\nu\bar{\nu}b\bar{b}$ ). To suppress the  $W$ +jets background, a cut to reject events with transverse mass  $m_T(l, E_T^{\text{miss}})$  (where  $l$  is the electron or the muon, and  $E_T^{\text{miss}}$  is the missing transverse momentum) compatible with the  $W$  boson are used by both the collaborations. Backgrounds from all processes that involve jets misidentified as  $\tau_{\text{had}}$  are estimated simultaneously in a data-driven fake-factor method. For  $W$ +jets, the fake factor is measured in a region identical to the signal region, but with reversed cut on  $m_T(l, E_T^{\text{miss}})$ . For multi-jet events, the fake factor is measured in a region defined by inverting the isolation requirement of the electron or muon for ATLAS collaboration, and by inverting the requirement on the relative charge of the  $\tau_{\text{had}}$  with respect to the electron or to the muon for the CMS collaboration. Events with electrons misidentified as a  $\tau_{\text{had}}$  are suppressed by the ATLAS collaboration with a veto on the visible mass of the  $\tau_{\text{had}}$  and lepton of the  $Z$  boson mass window,  $80 \text{ GeV} < m_{\text{vis}} < 110 \text{ GeV}$ , while the CMS collaboration vetoed events with containing a pair of opposite sign electrons or muons passing slightly looser identification and isolation conditions compared with the signal electrons/muons. Backgrounds with a correctly identified  $\tau_{\text{had}}$  are taken from simulation, with additional derived data/MC corrections.

Finally, for the  $\tau_e\tau_\mu$  channel by the CMS collaboration, the contribution from  $W$ +jets is small and taken from MC. For the multi-jet estimate, the with same sign ( $e, \mu$ ) data is used after subtracting all the other backgrounds. All the other backgrounds are taken from simulation, with additional derived data/MC corrections.

The transverse invariant mass of the ditau candidate pair,  $m_T(\tau_1, \tau_2)$ , is used to search for a possible signal contribution on top of the expected backgrounds by the CMS collaboration, while ATLAS used the total transverse mass, defined as  $m_T^{\text{tot}} = \sqrt{m_T^2(\tau_1, \tau_2) + m_T^2(\tau_1, E_T^{\text{miss}}) + m_T^2(\tau_2, E_T^{\text{miss}})}$ . For both the collaborations, the observed event yields are compatible with the expected event yield from SM processes, within uncertainties. The  $m_T(\tau_1, \tau_2)$  and  $m_T^{\text{tot}}$  distributions for representative signal regions are shown in Fig. 2.

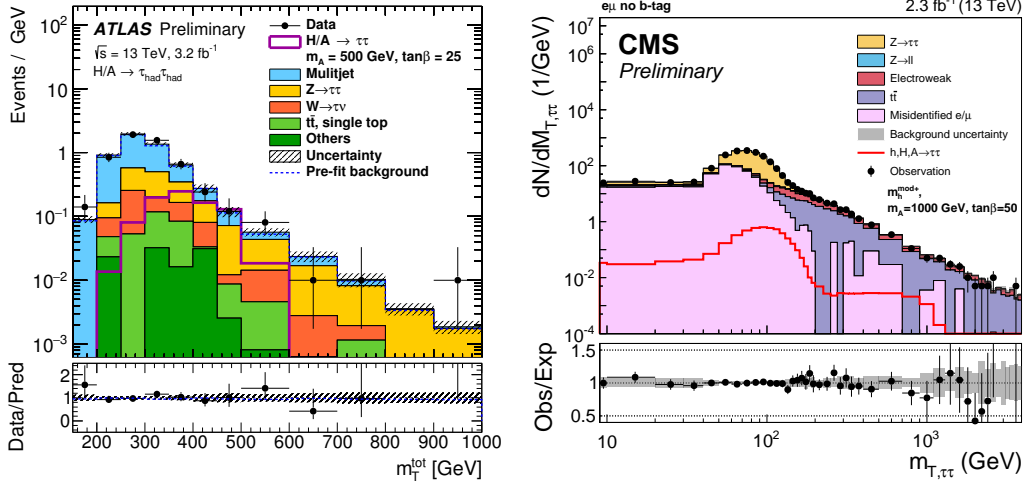


**Figure 2:** (Left) Post-fit plot of the total transverse mass distribution in the  $\tau_{\text{had}}\tau_{\text{had}}$  channel by the ATLAS collaboration. (Right) Post-fit plot of the transverse mass distribution in the no b-tag category of the  $\tau_e\tau_\mu$  channel by the CMS collaboration.

### 2.3 Results

The final result is provided both as a limit on the cross section times branching ratio as well as a model-dependent limit on various MSSM benchmark models. The limits for all channels combined are shown in Fig. 3 and Fig. 4 for the gluon fusion and b-associated production methods respectively, while Fig. 5 shows the expected and observed 95% CL upper limits on  $\tan\beta$  as a function of  $m_A$  in the MSSM  $m_h^{\text{mod}+}$  scenario, and the comparison with the LHC Run1 results. Already with the limited statistics recorded in 2015, the sensitivity exceeds the 8 TeV result for  $m_H > 750$  GeV for ATLAS and  $m_H > 350$  GeV for CMS.

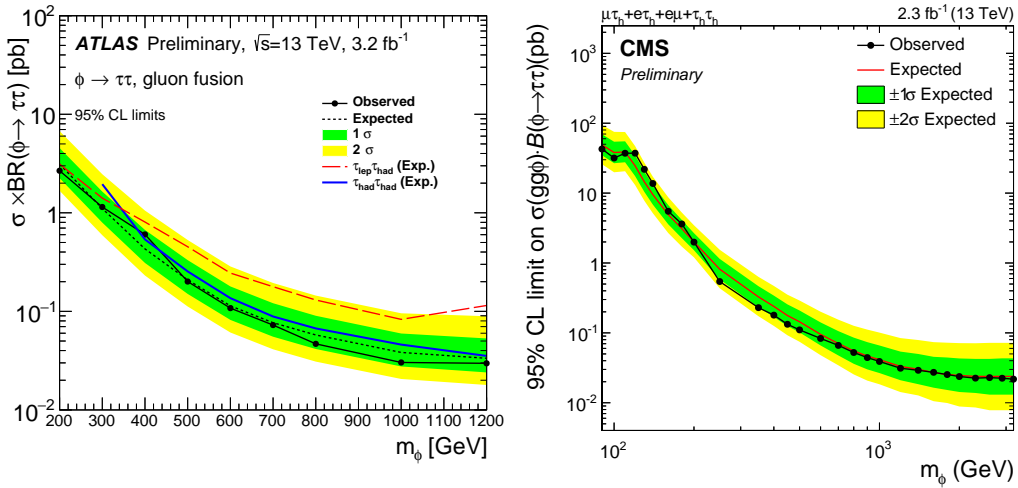


**Figure 3:** Observed and expected 95% CL upper limits on the product of cross section and the branching fraction  $\sigma(pp \rightarrow \phi) \times B(\phi \rightarrow \tau\tau)$  obtained by the ATLAS collaboration (left) and by the CMS collaboration (right) for the gluon-gluon fusion production.

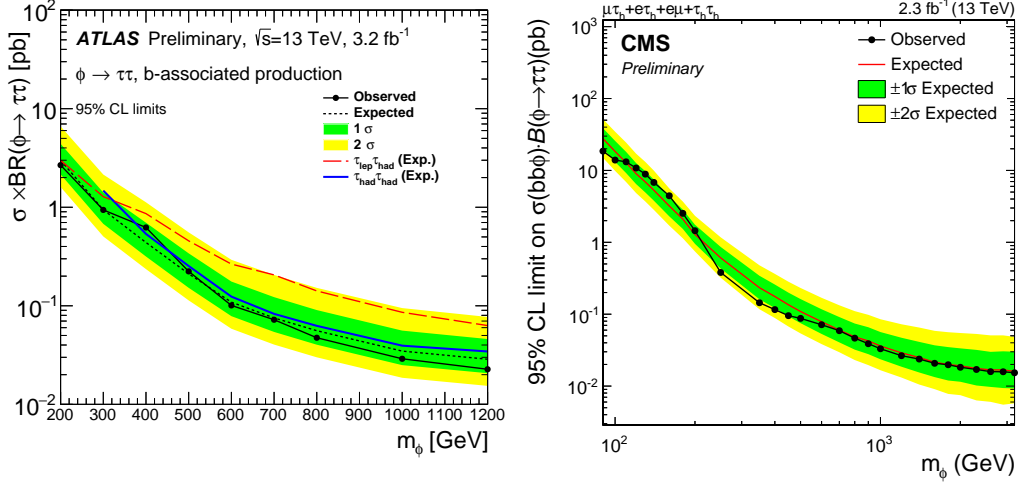


**Figure 4:** Observed and expected 95% CL upper limits on the product of cross section and the branching fraction  $\sigma(pp \rightarrow \phi) \times B(\phi \rightarrow \tau\tau)$  obtained by the ATLAS collaboration (left) and by the CMS collaboration (right) for the b-associated production.

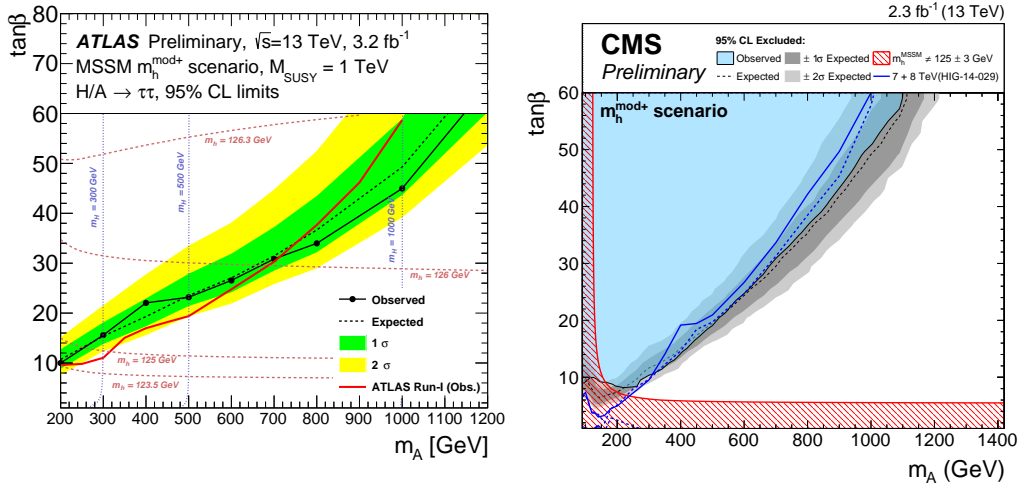


**Figure 5:** The expected and observed 95% CL upper limits on  $\tan\beta$  as a function of  $m_A$  in the MSSM  $m_h^{mod+}$  scenario for ATLAS (left) and CMS (right).

### 3. Search for Higgs boson pair production

The Higgs boson pair production could be used to investigate both the SM and the BSM scenarios.

Searches for *non-resonant*  $hh$  production give information on the trilinear coupling present in the SM Higgs potential fields; the same searches could spot out discrepancies with respect to the SM  $\lambda_{hhh}$  introduced by anomalous couplings and new physics.

Similar searches in the *resonant* regime could be used to explore the BSM world; new particles, introduced by extensions in the  $\mathcal{L}_{SM}$ , could decay in a couple of Higgs SM like boson (Di-Higgs). The experience acquired during the 8 TeV data taking period at LHC for SM Higgs search is used

for seek different final state configuration of the Di-Higgs.

In this paragraph an overview of the latest *resonant* results, provided by ATLAS and CMS experiment for 13 TeV collision, will be presented. Both collaboration have produced results with 8 TeV data [14][1] in many Di-Higgs decay configurations as shown in figure 6.

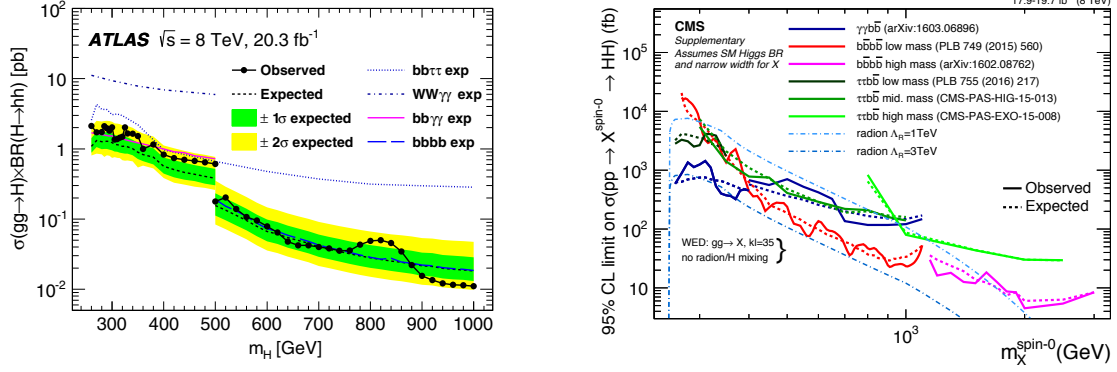


**Figure 6:** (left) ATLAS combination Higgs boson pair production in the  $hh \rightarrow bb\tau\tau, \gamma\gamma WW^*, \gamma\gamma bb, bbbb$  channels with 8 TeV data, (right) CMS Observed and expected 95% CL upper limits on the product of cross section and the branching fraction  $\sigma(gg \rightarrow X) \times B(X \rightarrow hh)$  obtained by different analyses assuming spin-0 hypothesis.

### 3.1 $H \rightarrow hh \rightarrow bbbb$ channel

The Higgs boson decay mode in b quarks has the highest branching ratio, this imply that a Di-Higgs final state, with each Higgs dacaying into a b pair, it's the most prominent one between the others. Although search of this kind of final state should take into account the overwhelming multi-jet background, largely produced at hadrons collider.

ATLAS and CMS collaborations analysis scan a mass range  $260 \text{ GeV} < m_H < 3000 \text{ GeV}$ , particularly CMS cover from  $260 \text{ GeV}$  to  $1200 \text{ GeV}$  and ATLAS from  $500 \text{ GeV}$  to  $3000 \text{ GeV}$ . Both analysis have different strategy for different  $m_H$  ranges: low-mass region ( $260 \text{ GeV} < m_H < 400 \text{ GeV}$ ), medium-mass ragion ( $400 \text{ GeV} < m_H < 1200 \text{ GeV}$ ), boosted region ( $1200 \text{ GeV} < m_H < 3000 \text{ GeV}$ ). The categorisation is chosen to maximise to significance of the analysis.

The results are shown in figure 7.

### 3.2 $H \rightarrow hh \rightarrow bb\tau\tau$ channel

The  $bb\tau\tau$  channel can exploit the presence of the  $\tau$  leptons to take care of the multi-jet back-ground.

The analysis performed by CMS collaboration scans a  $260 \text{ GeV} < m_H < 900 \text{ GeV}$  and combine three different  $\tau\tau$  final state:  $\mu\tau_h, e\tau_h$  and  $\tau_h\tau_h$ , where  $\tau_h$  stands for the hadronic decays of a  $\tau$ . The finale  $m_H$  shape is constructed using a dedicated kinematic fit procedure.

Observed and expected 95% CL upper limits are shown in figure 8.

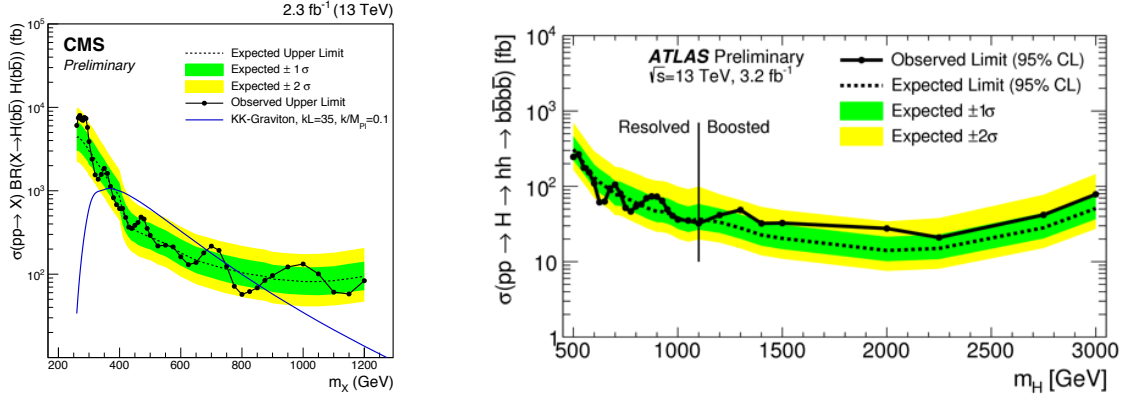


**Figure 7:** (left) CMS: The observed and expected upper limits on the cross section for a spin-2 resonance  $H \rightarrow hh \rightarrow bbbb$  at a 95% confidence level using data corresponding to an integrated luminosity of  $2.3 fb^{-1}$  at  $13 TeV$  using the asymptotic  $CL_S$  method, (right) ATLAS: The expected and observed upper limit for  $pp \rightarrow H \rightarrow hh \rightarrow bbbb$  with fixed  $\Gamma_H = 1 GeV$ , at the 95% confidence level .

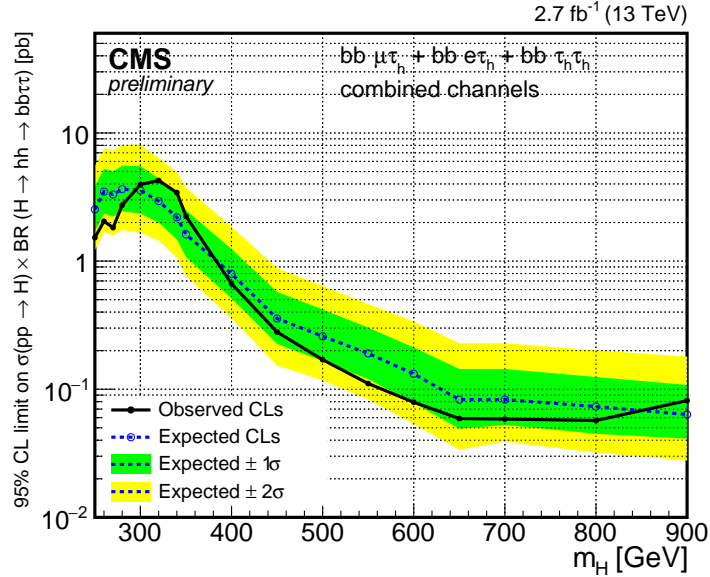


**Figure 8:** Observed and expected 95% CL upper limits on  $\sigma(pp \rightarrow H) \times BR(H \rightarrow hh \rightarrow bb\tau\tau)$  from the combination of the three channels as a function of the mass of the resonance  $m_H$

### 3.3 $H \rightarrow hh \rightarrow bbWW$ channel

The search for resonant Higgs pair production,  $H \rightarrow hh$ , where one of the  $h$  decays as  $h \rightarrow bb$ , and the other as  $H \rightarrow WW \rightarrow l'l'$  (where  $l$  is either an electron or a muon) is performed by CMS collaboration using LHC proton-proton collision data at  $13 TeV$ . The analysis focuses on the invariant mass distribution of the b-jet pair, searching for a resonant-like excess compatible with the  $h$  boson mass in combination with a boosted decision tree discriminant based on kinematic information. The dominant background is  $tt$  production with smaller contributions from Drell-Yan and single top processes. Figure 9 shows the result obtained.



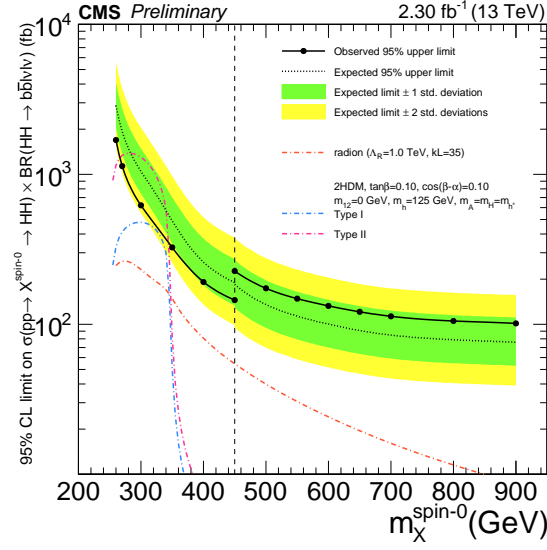


**Figure 9:** Observed and expected 95% CL upper limits on  $\sigma(pp \rightarrow H) \times BR(H \rightarrow hh \rightarrow bbl\nu l\nu)$

### 3.4 $H \rightarrow hh \rightarrow bb\gamma\gamma$ channel

The  $bb\gamma\gamma$  final state is particularly promising for the DiHiggs search, as it benefits from the large branching fraction of the  $h \rightarrow bb$  decay and the clean di-photon signal, due to high  $m_{\gamma\gamma}$  resolution, on top of a smooth continuum di-photon background from multi-jet and multi-photon SM processes.

The analysis performed by ATLAS collaboration scans masses in the range  $275\text{GeV} < m_H < 400\text{GeV}$ . A counting approach is adopted in order to estimate the number of signal and background events.

Observed and expected 95% CL upper limits are shown in figure 10.

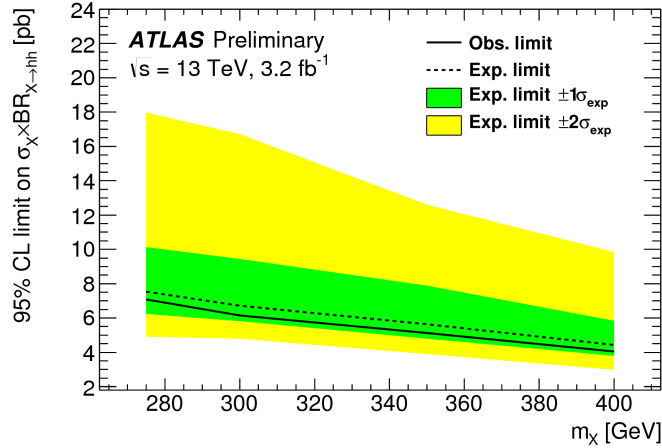


**Figure 10:** Observed and expected 95% CL upper limits on  $\sigma(pp \rightarrow H) \times BR(H \rightarrow hh \rightarrow bb\gamma\gamma)$

## 4. Conclusions

## References

- [1] Higgs pag summary plots. <https://twiki.cern.ch/twiki/bin/view/CMSPublic/SummaryResultsHIG>.
- [2] Search for Neutral Minimal Supersymmetric Standard Model Higgs Bosons  $H/A \rightarrow \tau\tau$  produced in  $pp$  collisions at  $\sqrt{s} = 13$  TeV with the ATLAS Detector. Technical Report ATLAS-CONF-2015-061, CERN, Geneva, Dec 2015.
- [3] Search for a doubly-charged Higgs boson with  $\sqrt{s} = 8$  TeV  $pp$  collisions at the CMS experiment. Technical Report CMS-PAS-HIG-14-039, CERN, Geneva, 2016.
- [4] Search for Higgs boson pair production in the  $b\bar{b}\gamma\gamma$  final state using  $pp$  collision data at  $\sqrt{s} = 13$  TeV with the ATLAS detector. Technical Report ATLAS-CONF-2016-004, CERN, Geneva, Mar 2016.
- [5] Search for resonant Higgs boson pair production in the  $b\bar{b}\tau^+\tau^-$  final state. Technical Report CMS-PAS-HIG-16-013, CERN, Geneva, 2016.
- [6] Search for resonant Higgs boson pair production in the  $b\bar{b}l\nu l\nu$  final state at  $\sqrt{s} = 13$  TeV. Technical Report CMS-PAS-HIG-16-011, CERN, Geneva, 2016.
- [7] Search for resonant pair production of Higgs bosons decaying to two bottom quark-antiquark pairs in proton-proton collisions at 13 TeV. Technical Report CMS-PAS-HIG-16-002, CERN, Geneva, 2016.
- [8] Summary results of high mass BSM Higgs searches using CMS run-I data. Technical Report CMS-PAS-HIG-16-007, CERN, Geneva, 2016.
- [9] Morad Aaboud et al. Search for charged Higgs bosons produced in association with a top quark and decaying via  $H^\pm \rightarrow \tau\nu$  using  $pp$  collision data recorded at  $\sqrt{s} = 13$  TeV by the ATLAS detector. *Phys. Lett.*, B759:555–574, 2016.
- [10] Morad Aaboud et al. Search for charged Higgs bosons produced in association with a top quark and decaying via  $H^\pm \rightarrow \tau\nu$  using  $pp$  collision data recorded at  $\sqrt{s} = 13$  TeV by the ATLAS detector. *Phys. Lett.*, B759:555–574, 2016.
- [11] Morad Aaboud et al. Search for pair production of Higgs bosons in the  $b\bar{b}b\bar{b}$  final state using proton–proton collisions at  $\sqrt{s} = 13$  TeV with the ATLAS detector. 2016.
- [12] G. Aad and etal. Constraints on new phenomena via higgs boson couplings and invisible decays with the atlas detector. *Journal of High Energy Physics*, 2015(11):1–52, 2015.
- [13] Georges Aad et al. Search for new phenomena in events with at least three photons collected in  $pp$  collisions at  $\sqrt{s} = 8$  TeV with the ATLAS detector. *Eur. Phys. J.*, C76(4):210, 2016.
- [14] ATLAS Collaboration. Searches for higgs boson pair production in the  $hh \rightarrow b\bar{b}\tau\tau, \gamma\gamma W^*, \gamma\gamma b\bar{b}, b\bar{b}b\bar{b}$  channels with the atlas detector. *Phys. Rev. D*, 92:092004, Nov 2015.
- [15] V. Khachatryan and etal. Search for a charged higgs boson in  $pp$  collisions at  $\sqrt{s} = 8$ tev. *Journal of High Energy Physics*, 2015(11):1–64, 2015.
- [16] V. Khachatryan and etal. Search for neutral mssm higgs bosons decaying into a pair of bottom quarks. *Journal of High Energy Physics*, 2015(11):1–43, 2015.
- [17] V. Khachatryan and etal. Search for neutral mssm higgs bosons decaying to  $\mu^+\mu^-$  in  $pp$  collisions at. *Physics Letters B*, 752:221 – 246, 2016.